

# Building velocity model for anisotropic PSDM: A TTI modeling example

Lanlan Yan, Larry R. Lines and Don C. Lawton - Fold-Fault Research Project, University of Calgary

CSEG Geophysics 2002

## Abstract

Steeply dipping shale and interbedded sandstone and shale formations in fold and thrust belt areas, such as Alberta Rocky Mountain Foothills, exhibits seismic velocity anisotropy. Transverse isotropy with a tilted symmetry axis (TTI medium) has been recognized as a major anisotropic feature of shale formation in the Western Canada sedimentary basin. Since TTI medium in the overburden of subsurface targets mis-positions the lateral and vertical locations of hydrocarbon on the conventional isotropic depth image, it is important to be able to build a velocity model for anisotropic pre-stack depth migration (PSDM). In this paper, we construct a TTI model, which is a simplified version of a typical overthrust section from the Alberta Foothills. The velocity model includes a 1500 m layer of varied dipping transversely isotropic beds mainly composed of Cretaceous shale and sandstone, and a deeper anticlinal target made of Mississippian carbonate. We generate anisotropic seismic data sets by employing NORSAR2D ray tracing package. With the assumption that TTI layer is homogeneous and the symmetry axis is perpendicular to its beddings, we estimate anisotropic velocity model ( $V_0$ ,  $\theta$ ,  $\epsilon$ ,  $\delta$ ) with the integration of standard normal-moveout (NMO) analysis and isotropic migration velocity analysis. Specifically, we invert P-wave NMO velocities and zero-offset traveltimes for the symmetry direction velocity  $V_0$  (also called slow velocity) and Thomsen's anisotropic parameter  $\delta$ . Another Thomsen's parameter  $\epsilon$  is obtained using parameter scanning technique constrained by isotropic migration velocity analysis. The dips of anisotropic strata,  $\theta$ , are derived by either isotropic PSDM or zero-offset traveltime from isotropic migration velocity analysis. Our estimates of  $V_0$ , Thomsen's anisotropic parameters,  $\epsilon$  and  $\delta$  are close to their actual values. The error bars in the inversion and derivation are probably associated with the uncertainties in picking velocities in NMO analysis and picking zero-offset traveltimes in isotropic migration velocity analysis.

## Introduction

The structural geology in the Alberta Rocky Mountain Foothills is primarily dominated by thrust faults, complex folds and steeply dipping formations. In these fold and thrust belt areas, the hydrocarbon reservoirs are frequently overlain by thick, dipping shales and thinly interbedded sandstones and shales. Shales exhibit seismic velocity anisotropy, which refers to the variation of velocity with direction, with the main symmetry axis perpendicular to bedding (Johnston and Christensen, 1995). The main physical reasons of seismic anisotropy are due to aligned mineral grains, aligned cracks, aligned crystals and periodic thin layering (Helbig, 1994). In the Western Canada sedimentary basin, especially in Foothills, velocity anisotropy is likely to exist in interbedded shales and sandstones, where folding and faulting can thrust these stratigraphic horizons to the surface with steep dip angles. The structural character above often makes seismic velocity anisotropy give rise to TI medium with a tilted symmetry axis (called here TTI). TTI model is very typical for overthrust areas in Canadian Foothills, where TI shale layers are often bent and thrust to the surface due to tectonic processes and the dips may exceed 45 degree (Leslie and Lawton, 1996; Grechka, et al., 2001).

The presence of TTI medium in overthrust areas may produce severe imaging problems, such as mis-positioning and mis-focusing of exploration targets if anisotropic influence is not considered in the conventional velocity analysis and standard prestack depth migration techniques. Not only the deeper are poorly focussed and mis-positioned, these events beneath dipping anisotropic beds will be also shifted updip and produce time pull-up in the isotropic PSDM section. Fortunately, Leslie and Lawton (1998) and Vestrum et al. (1999) showed some successful applications of anisotropic PSDM on both model and field data sets. In their examples, higher-quality images of both dipping and horizontal features in the overthrust areas are produced by PSDM algorithms capable of handling TTI medium. Anisotropic PSDM corrects for lateral shifts, correctly positions events in depth, and properly focuses diffraction energy.

In reality, evaluating anisotropic parameters suitable for performing anisotropic PSDM is a very challenging project, especially from surface seismic data in structurally complicated areas. Thomsen's anisotropic parameters  $\epsilon$  and  $\delta$  are two important coefficients governing P-wave velocity behaviour.  $\epsilon$  is the fractional difference between velocities parallel and perpendicular to the bedding (equation (1)).  $\delta$  is proportional to the difference between P-wave velocity oblique to bedding and  $V_0$  (equation (2)).  $\delta$  is an important parameter when dealing with anisotropic layers with zero dip because it causes the non-hyperbolic moveout effect due to anisotropy.

$$\epsilon = (V_{90} - V_0) / V_0 \quad (1)$$

$$\delta = 4 * [(V_{45} / V_0) - 1] - \epsilon \quad (2)$$

In general, anisotropic parameters can be measured by laboratory experiments (Banik, 1984; Vernik and Liu, 1997; Lo et al., 1986; Thomsen, 1986; Levin, 1990). Survey seismic such as refraction survey and multi-channel VSP can also be employed to derive  $\epsilon$  and  $\delta$  through calculating velocities at different directions such as  $V_{90}$ ,  $V_{45}$  and  $V_0$  (Leslie and Lawton, 1999). We can also integrate well logs (interval velocity) and surface seismic (root-mean square velocity) to approximate  $\epsilon$  and  $\delta$  parameters (Alkhalifah et al., 1995. Isaac and Lawton (2000) proposed a practical estimation of anisotropic parameters from surface P-wave seismic data. Their method was based on inversion of three values, zero-offset arrival time, the difference in arrival time between a near-offset and a far-offset and the difference in imaged location observed at these offsets. Grechka et al. (2001) showed anisotropic velocity analysis for TTI on a physical modeling data set (Leslie and Lawton, 1996) by inverting P-wave NMO velocities and zero-offset traveltimes for the slow velocity  $V_0$  and the anisotropic parameters  $\epsilon$  and  $\delta$ .

Quite similar to the physical model generated by Leslie and Lawton (1996), we construct a TTI model with varied dipping transversely isotropic beds. The only difference between this numerical model and the physical model is that the underlain carbonate reservoir is a small anticlinal target instead of a flat layer. The objective of this study is to investigate the feasibility of anisotropic velocity analysis and imaging in overthrust areas by integrating the NMO velocities inversion and isotropic migration velocity analysis.

### Numerical TTI modeling

A 2-D numerical TTI model is constructed to simulate anisotropic thrust sheet in overthrust structures typical for Alberta Rocky Mountain Foothills (shown in Figure 1). Four blocks make up a bending TTI layer with the symmetry axis (marked with black arrows) perpendicular to the bedding. The varied dips of the anisotropic blocks are 0, 30, 45, 60 degrees, respectively. The P-wave velocities in the slower direction ( $V_0=3500$  m/s) and in the fast direction ( $V_{90}=4200$  m/s) yield the anisotropic parameters  $\varepsilon=0.20$  and  $\delta=0.05$ . The TTI layer is embedded in a purely isotropic environment with the P-wave velocity overlain of it equals 3020 m/s and the P-wave velocity underlain of it equals 3960 m/s. Our hydrocarbon reservoir is a small anticline with the target height at the offset of 5.0 km laterally and 4.0 km in the depth vertically. Anisotropic seismic data sets are generated by ray tracing package in NORSAR-2D. The acquisition parameters in NORSAR-2D are as follows: total CMP points of 762, CMP interval of 12.5m, group interval of 25m, minimum offset of 0m, and maximum offset of 2500m. A Ricker zero-phase wavelet with the frequency of 30 Hz is used in the model data.

To apply the theory of Grechka and Tsvankin (1999) to perform a parameter-estimation from surface P-wave data, we make similar assumptions to those of Grechka et al. (2001) in trying to avoid inversion ambiguities in the model parameter estimations. They are: (1) Four blocks making up the TTI layer in Figure 1 are homogeneous; (2) The four anisotropic blocks are made of the same material ( $\varepsilon$  and  $\delta$  are evenly uniformed everywhere) with the symmetry axis perpendicular to the boundary within each block; (3) The surrounding rocks of the TTI thrust sheet are isotropic; (4) The anticlinal target is symmetric laterally in the deeper section.

### Inversion for the anisotropic parameters

Under the assumption made above, it is possible to estimate model parameters ( $V_0$ ,  $\theta$ ,  $\varepsilon$ ,  $\delta$ ) in the depth domain by the integration of NMO velocities inversion and isotropic migration velocity analysis based on the curvature measurement and stacking power (Yan, Lines and Lawton, 2001). As seen in Figure 2a, we describe the numerical TTI model as primarily three layers. We start with seismic event R3 (Figure 2b) reflected from isotropic layer 3 in segment B. The two-way zero-offset traveltimes  $\tau_{R3}$  and NMO velocity  $V_{nmo, R3}$  can be picked on semblance panel of Figure 2b. Since layer 3 in segment B is completely flat, the zero-offset traveltimes  $\tau_{R3}$  and NMO velocity  $V_{nmo, R3}$  from conventional NMO analysis are exactly equivalent to the physical meanings of zero-offset traveltimes and interval velocity of isotropic layer 3. Through calculating the average values of the zero-offset traveltimes  $\tau_{R3}$  and NMO velocity  $V_{nmo, R3}$  over at least 8 super CMP gathers, we get  $\tau_{R3}=2.2734$  s and  $V_{nmo, R3}=V_{in, R3}=4023$  m/s. The depth of layer 3 around segment B and segment A should be a constant based on assumption (4) and is computed as  $Z=Z_{R3}=\tau_{R3} \cdot V_{in, R3} / 2=4.572$  km.

Repeating the same procedure above, we pick zero-offset traveltimes and NMO velocities of Layers 1 and 2 from Figure 2c. Event R1 is seismic reflection from the bottom of the isotropic layer1; therefore in segment A, the NMO velocity  $V_{nmo, R1}=V_{in, R1}=3057$  m/s and zero -offset traveltimes  $\tau_{R1}=1.3222$  s. The estimated thickness of layer 1 in segment A is  $Z=Z_{R1}=\tau_{R1} \cdot V_{in, R1} / 2=2.021$  km. Event 2, reflected from the bottom of VTI block (shown in Figure 2c), contains important information about the NMO velocity  $V_{nmo}$  in the TTI layer. Anisotropic block defined by segment A between layers 1 and 2 is VTI symmetry and  $V_{nmo}$  can be related to the symmetry-direction velocity or slow velocity  $V_0$  as shown by Thomsen (1986)

$$V_{nmo} = V_0 \sqrt{1 + 2\delta} \quad (3)$$

Since we assume all anisotropic blocks are homogeneous, the interval NMO velocity  $V_{nmo}$  can be obtained using the conventional Dix (1955) differentiation:

$$V_{nmo} = \sqrt{(\tau_{R2} V_{nmo, R2}^2 - \tau_{R1} V_{nmo, R1}^2) / (\tau_{R2} - \tau_{R1})} = 3784 \text{ m/s} \quad (4)$$

where  $\tau_{R2}=2.1816$  s and  $V_{nmo, R2}=3361$  m/s are the picked zero-offset traveltimes and NMO velocity for reflected event 2 (Figure 2c) of layer 2 in segment A. With the difference of zero-offset traveltimes of layers 3 and 2, we compute the interval thickness between layers 2 and 3 with the value of  $DZ_{R2, R3}=(\tau_{R3} - \tau_{R2}) \cdot V_{in, R3} / 2=1.015$  km. Under assumption (4), the depth of layer 3 in segment B is equal to depth of layer 3 in segment A; therefore the vertical velocity  $V_0$  in VTI block can be computed as

$$V_0 = 2(Z_{R3} - Z_{R1} - DZ_{R2, R3}) / (\tau_{R2} - \tau_{R1}) = 3574 \text{ m/s} \quad (5)$$

Then, applying equation (3), we obtain anisotropic parameter  $\delta=0.0602$ . As a result, the conventional NMO velocities and zero-offset traveltimes in VTI block (the left edge of TTI model) are employed to invert the parameters of the TTI layer: the symmetry-direction velocity  $V_0$  and the Thomsen's anisotropic parameter  $\delta$ .

When we assume that we do not know the subsurface medium is anisotropic, we perform standard isotropic PSDM trying to obtain the dips of thrust sheet. With the assumption that TTI layer has a uniform thickness along the four blocks, the dips of TTI layer can be determined using isotropic PSDM after standard isotropic migration velocity analysis (Yan, Lines and Lawton, 2001) on the isotropic layer 1. Figure 2d shows the estimated dips of the anisotropic model. Constrained by the best velocity value of TTI layer ( $V_{in, R2}=3856$  m/s) estimated

from the standard isotropic velocity analysis, an optimum anisotropic parameter  $\epsilon$  ( $\epsilon=0.1910$ ) is acquired using parameter scanning technique in the procedure of anisotropic PSDM. Table 1 compares the actual values and inverted values of the symmetry-direction velocity and anisotropic parameters.

### Prestack depth migration results

Based on the actual and estimated anisotropic velocity models ( $V_0, \theta, \epsilon, \delta$ ), both isotropic PSDM and anisotropic PSDM are performed intending to compare the image results and highlight the serious image problems such as mis-positioning and mis-focussing of TTI layer from using conventional isotropic migration algorithm. Figure 3 is the image result of isotropic PSDM. Although the true vertical velocity model, the image of the bottom layer of TTI medium is mis-focussing and the deeper anticline, our hydrocarbon reservoir, is obviously mis-positioned. The blurred image of the target high makes seismic interpretation to be difficult and increases the exploration risks. Figures 4 and 5 show two images of anisotropic PSDM using actual anisotropic velocity model and estimated anisotropic velocity field. The image comparisons among three figures emphasise the advantages of anisotropic migration algorithm capable of handling TTI medium; particularly, the target high from anisotropic PSDM in Figures 4 and 5 is shifted along the down-dip direction toward its true spatial location. The lateral shift is in the order of 125 meter and vertical shift is around 75 meter. In addition, the similar and quite comparable images between Figures 4 and 5 demonstrate the principal feasibility of anisotropic velocity analysis and imaging in overthrust areas.

### Discussion and conclusions

The presence of TTI media yields serious image distortions by singular conventional migration velocity analysis and imaging in complicated overthrust area. The proposed anisotropic velocity analysis based on integrating inversions of NMO velocities and zero-offset traveltimes and standard isotropic MVA is effective in reconstructing anisotropic velocity model ( $V_0, \theta, \epsilon, \delta$ ). The comparable anisotropic PSDM images using the actual model and the estimated field demonstrate the feasibility of this technique on this specific numerical TTI model. To address the issues of ambiguities in parameter inversions, some important constraints on the numerical TTI model are provided by the geologically justified assumptions that the symmetry axis is perpendicular to the boundaries and the TTI layer is homogeneous. Although these assumptions are relatively simple and the proposed approach is somewhat subjective or limited by the assumptions associated, it can still provide useful information and insight regarding the uncertainties in parameter inversions for anisotropic media.

### Acknowledgement

We thank Dr. Helen Isaac at Fold and Fault Research Project, University of Calgary for providing help in seismic acquisition on numerical TTI model in NORSAR-2D and anisotropic PSDM tests in Sage processing package.

### References

Alkhalifah, T., and Tsvankin, I., 1995, Velocity analysis for transversely isotropic media: *Geophysics*, **60**, 1550-1566.  
 Banik, N. C., 1984, Velocity anisotropy of shales and depth estimation in the North Sea basin: *Geophysics*, **49**, 1411-1419.  
 Dix, C. H., 1955, Seismic velocities from surface measurements: *Geophysics*, **20**, 68-86.  
 Grechka, V., Pech, A., Tsvankin I., and Han B., 2001, Velocity Analysis for tilted transversely isotropic media: A physical

Modeling example: *Geophysics*, **66**, 904-910.  
 Helbig, K., 1994, Foundations of anisotropy for exploration seismics: Pergamon.

Isaac, J. H., and Lawton D. C., 2000, A new method for the estimation of anisotropy parameters from surface P-wave seismic data: 70<sup>th</sup> Ann. Internat. Mtg. Soc. Explor. Geophys., Expanded Abstract  
 Leslie, J. M., and Lawton, D. C., 1999, A refraction-seismic field study to determine the anisotropic parameters of shales: *Geophysics*, **64**, 1247-1252.  
 Leslie, J. H., and Lawton, D. C., 1996, Structural imaging below dipping anisotropic layers: Predictions from seismic modeling: 66<sup>th</sup> Ann. Internat. Mtg., Soc. Expl. Geophys., Expanded Abstract, 719-722.  
 \_\_\_\_\_, 1998, Anisotropic pre-stack depth migration: The Recorder, **23**, No. 10, 23-36.  
 Levin, F., 1990, Reflections from a dipping plane-Transversely anisotropic solid: *Geophysics*, **55**, 851-855.  
 Lo, T.-W., Coyner, K. B., and Toksöz, M.N., 1986, Experimental determination of elastic anisotropy of Berea sandstone, Chicopee shale, and Chelmsford granite: *Geophysics*, **51**, 164-171.  
 Johnston, J.E., and Christensen, N.I., 1994, Elastic constants and velocity surfaces of indurated anisotropic shales: *Surveys in Geophysics*, **15**, 481-494.  
 Vernik, L., and Liu, X., 1997, Velocity anisotropy in shales: A petrophysical study: *Geophysics*, **62**, 521-532.  
 Thomsen, L., 1986, Weak elastic anisotropy: *Geophysics*, **51**, 1954-1966.  
 Vestrum R. W., Lawton D. C., and Schmid, R., 1999, Imaging structures below dipping TI media: *Geophysics*, **64**, 1239-1246.  
 Yan, L., Lines, L. R., and Lawton, D. C., 2001, Migration velocity analysis by curvature measurement and stacking power: 71<sup>th</sup> Ann. Internat. Mtg., Soc. Expl. Geophys., Expanded Abstract, MIG 1.1.

**Figure 1.** Numerical model of TTI layer, the symmetry axis (marked by black arrows) is perpendicular to the layer boundaries.

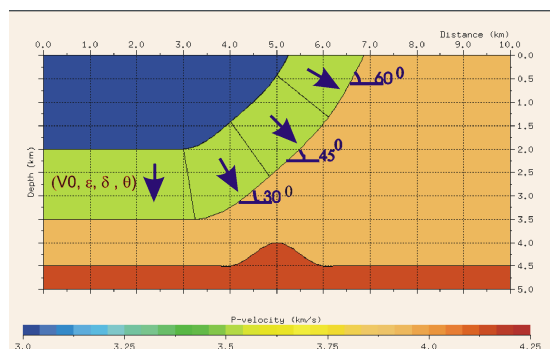


**Table 1.** Comparison of actual and inverted anisotropic models.

Actual parameters	Estimated parameters(*)
$V_0=3500$ m/s, $\epsilon=0.20$	$V_0^*=3574$ m/s, $\epsilon^*=0.1910$
$\delta=0.05$	$\delta^*=0.0602$

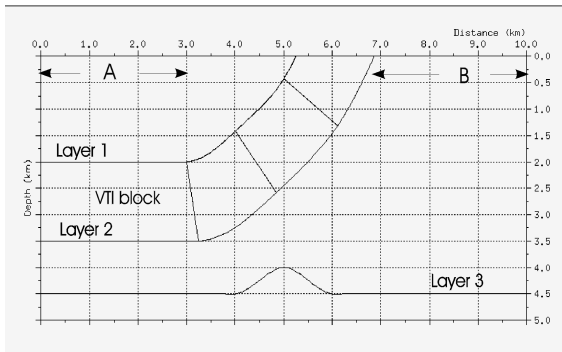


Figure 2a. The layout of TTI model with three layers defined.

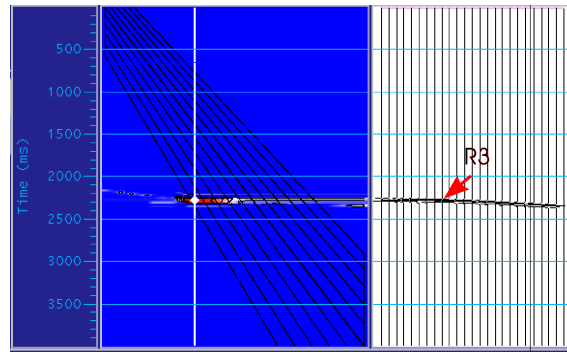


Figure 2b. NMO velocity analysis panel of event 3.

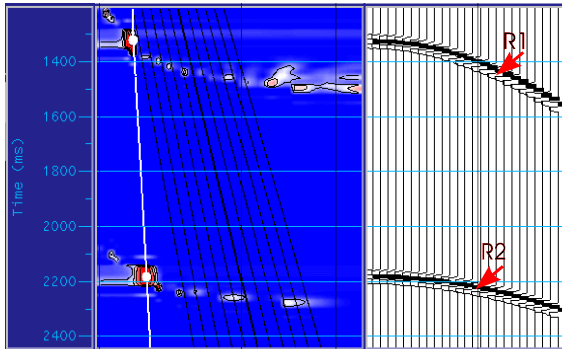


Figure 2c. NMO velocity analysis panel of events 1 and 2.

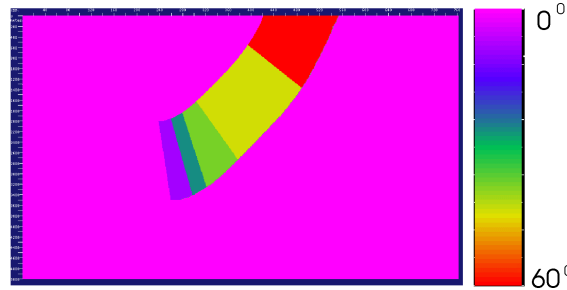


Figure 2d. The estimated dips of anisotropic field.

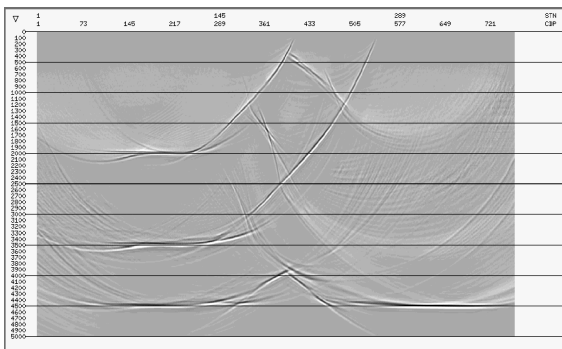


Figure 3. Prestack depth image from isotropic PSDM.

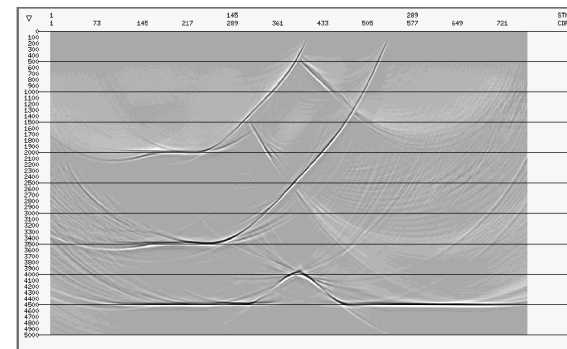


Figure 4. Anisotropic PSDM using true anisotropic model.

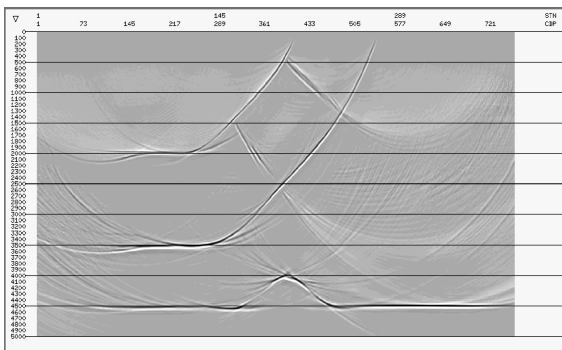


Figure 5. Anisotropic PSDM using estimated anisotropic field.